Online Supplement:

Leaf economics of early- and late-successional plants,

Appendices B-D

Jeremy W. Lichstein[1,*]

Brandon T. Peterson[2]

Jessica Langebrake[1]

Scott A. McKinley[2,3]

1. University of Florida, Department of Biology, Gainesville, FL 32611;

2. University of Florida, Department of Mathematics, Gainesville, FL 32601;

3. Tulane University, Department of Mathematics, New Orleans, LA 70118;

∗ Corresponding author; e-mail: jlichstein@ufl.edu.

Appendix B.   Mortality Assumptions

Overview

Here, we demonstrate that our main results are insensitive to variation in the whole-plant mortality rate (μ in eq. [A1]), including differences in μ between early- and late-successional species. We consider cases with constant μ (either a single value, or different values for early- and late-successional species) and cases where μ depends on a species' investment in structural leaf mass (LMA_s). In all cases we examined, and for a wide range of parameter values, the traits (LMA_p and LMA_s) of the most competitive ('optimal') early-successional species were predicted to be distinct from those of the optimal late-successional species. Furthermore, unless μ is implausibly large, the optimal values of LMA_p and LMA_s are qualitatively similar to those presented in the main text (fig. 1). Therefore, the main results and conclusions derived from our model appear robust to different assumptions concerning whole-plant mortality rates. It is possible that alternative mortality assumptions, beyond those we explored, could yield different results. However, the cases we describe below do not appear overly restrictive, and we speculate that our model results would be robust to a variety of alternative mortality assumptions.

Constant mortality rates

We first consider cases with constant μ (i.e., cases where μ is a fixed parameter, independent of other model parameters). Although the traits of the optimal late-successional species depend strongly on μ, those of the optimal early-successional species are independent of μ. This is illustrated in figures B1-B4, which show how the results in main-text figure 1 (where both early- and late-successional species have $\mu = 0.02$ yr^{-1}) change as μ increases. Note that the fraction of biomass that dies each year is $1 - e^{-\mu}$, so the values of μ in figures B1-B4 (0.02, 0.2, 2, and 40 yr^{-1}) correspond to annual biomass turnover percents of roughly 2%, 18%, 86%, and 100%, respectively.

The dependence of the optimal late-successional traits on μ, and the independence of the optimal early-successional traits, follow from the mathematical analyses of optimal trait values presented in Appendix D. In the late-successional case, μ has non-additive interactions with LMA_p and LMA_s (e.g., see eq. [D14]). In contrast, in the early-successional case, μ has a linear and non-interactive role (e.g., see eq. [D22]). Independence of the optimal early-successional traits from μ does not imply that the model dynamics are independent of μ. On the contrary, as μ increases (and all else being equal), biomass in our model (at any point in succession) decreases. Independence of the optimal early-successional traits from μ only means that the values of LMA_p and LMA_s that maximize biomass growth under full-sun conditions do not depend on μ.

As μ increases, the optimal late-successional traits become increasingly similar to the optimal early-successional traits. However, the optimal early- and late-successional traits are clearly distinct even if μ is as high as 2 yr^{-1} (fig. B3), corresponding to an annual biomass turnover of about 86% yr^{-1}. The late-successional solution converges on the early-successional solution only for $\mu > 10$ (e.g., fig. B4, where $\mu = 40$ yr^{-1} corresponds to an annual biomass turnover greater than 99.99% yr^{-1}). Even shade-intolerant tree species typically have mortality rates lower than 20% yr^{-1} (Davies, 2001; Poorter and Bongers, 2006; Wright et al., 2010), with community-mean turnover rates typically in the range of 1-5% yr^{-1} (e.g., Stephenson et al., 2011). Thus, realistic tree turnover rates are far lower than the values of μ required to blur the distinction between optimal early- and late-successional species in our analysis. Since the optimal early-successional traits are independent of μ, the above statements hold if μ is constant across species or if μ is a different constant for early- vs. late-successional species.

Mortality rate decreases with structural leaf mass investment

Late-successional tree species tend to have lower mortality rates than early-successional species (Connell and Slatyer, 1977; Pacala et al., 1996; Poorter and Bongers, 2006; Wright et al., 2010). The constant μ cases described above address cases where late-successional species have a higher fixed μ than early-successional species, but do not allow for explicit dependence of μ on other

traits. One way to accommodate this dependence is to assume that μ decreases with increasing LL, because LL tends to be higher for shade-tolerant late-successional species than for shade-intolerant early-successional species (Poorter and Bongers, 2006; Reich et al., 1995). In our model, LL is assumed to increase with LMA_s (eq. [A2]), and LMA_s is predicted to be higher for late-successional than for early-successional species (fig. 1). Thus, in our analysis, where we allow for only two species-specific parameters (LMA_p and LMA_s), we can explicitly link μ to a species' successional niche by assuming decreasing μ with increasing LMA_s.

We have no strong *a priori* grounds for determining the functional form for the relationship between μ and LMA_s, and so we choose a form that is mathematically convenient. Specifically, we assume that

$$\mu = m_1 + \frac{1}{m_2 LMA_s} \tag{B1}$$

and we explored different values of the parameters m_1 and m_2. This form is convenient because, as shown below, it is equivalent to a reparameterization of the constant μ case analyzed in Appendix D. Thus, we can rely on the analyses presented in Appendix D to study the behavior of the case where μ decreases with LMA_s according to equation (B1).
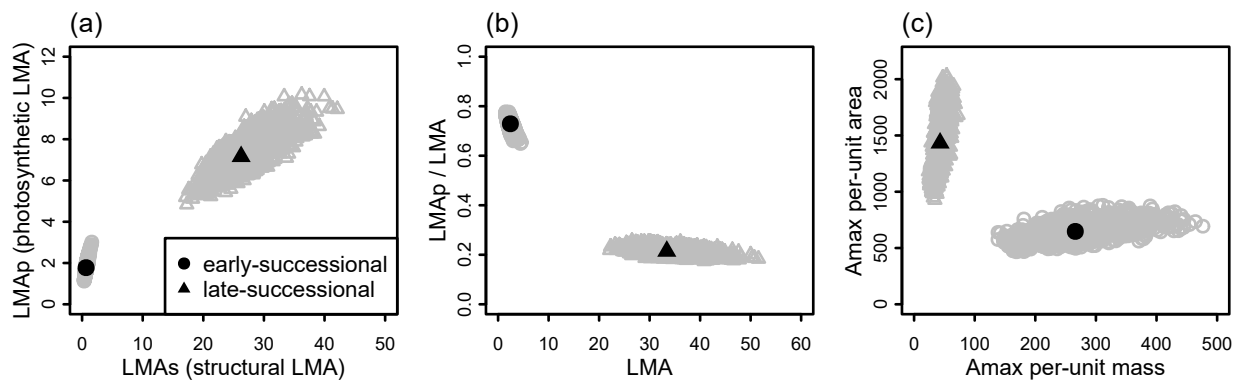

Figure B1: This figure is identical to main-text figure 1. Results are for the case where early- and late-successional species have a fixed mortality rate of $\mu = 0.02$ yr^{-1}.
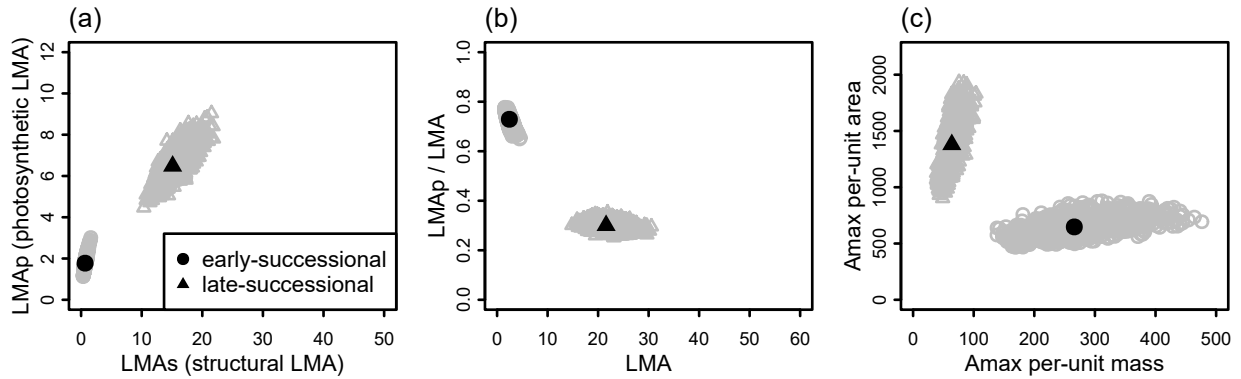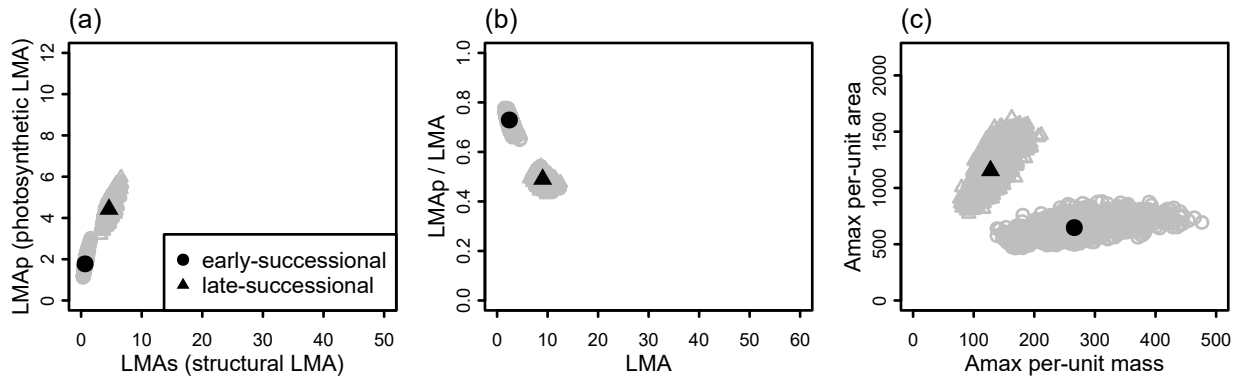
Figure B2: Same as figure B1, but with $\mu = 0.2$ yr^{-1}.

Figure B3: Same as figure B1, but with $\mu = 2$ yr^{-1}.

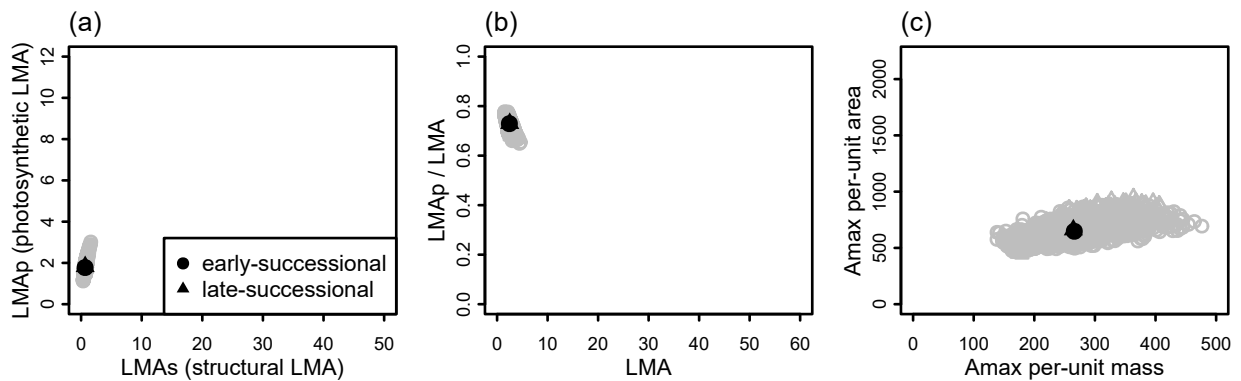Figure B4: Same as figure B1, but with $\mu = 40$ yr^{-1}.

To see that equation (B1) leads to a mathematically equivalent form of our model as the constant μ case, note that in the constant μ case, the total loss rate in equation (A1) is $\mu + LL^{-1} = \mu + 1/(c_{LL}LMA_s)$, where $LL = c_{LL}LMA_s$ (eq. [A2]); and for equation [B1], the total loss rate is $\mu + LL^{-1} = m_1 + 1/(m_2 LMA_s) + 1/(c_{LL}LMA_s) = m_1 + 1/(\theta LMA_s)$, where $\theta \equiv c_{LL}m_2/(c_{LL} + m_2)$. These two loss rates share the same mathematical form, so we can analyze the equation (B1) case using the same methods as described in Appendix D (constant μ case) by substituting m_1 for μ, and θ for c_{LL}.
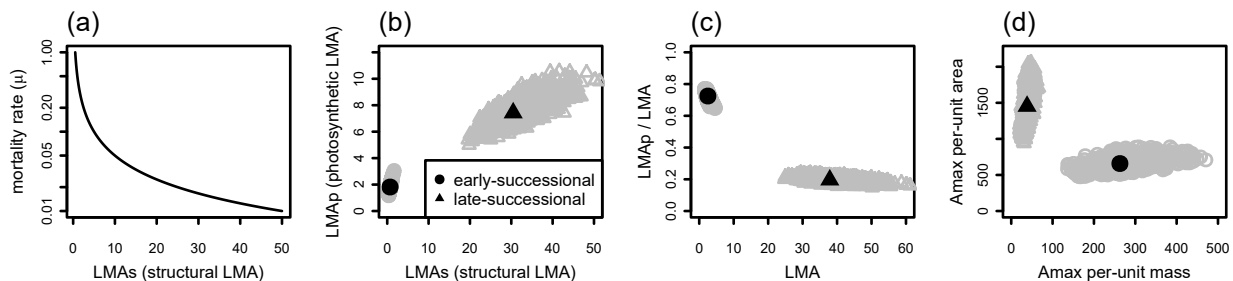

Figure B5: Results as in figures 1 and B1-B4, but for the case where μ decreases with LMA_s according to equation (B1) with parameter values $m_1 = 0$ and $m_2 = 2$. Panel (a) shows equation (B1), and panels (c-d) are as in figures 1 and B1-B4.
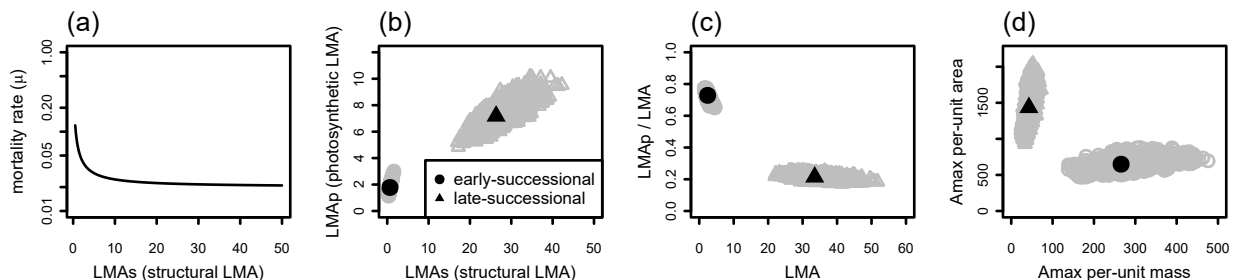
Figure B6: Same as figure B5, but with equation (B1) parameter values $m_1 = 0.02$ and $m_2 = 20$.

We explored a range of parameter values for m_1 and m_2, which determine the shape of the relationship between μ and LMA_s (compare figs. B5a and B6a). The examples presented in figures B5-B6 show that our main results (e.g., the clear difference in optimal traits between early- and late-successional species) are insensitive to the shape of equation (B1). The optimal early-

successional traits depend very weakly on the shape of equation (B1), with the early-successional values differing slightly between figures B5 and B6. The optimal late-successional traits depend more strongly on the shape of equation (B1). But for any choices of m_1 and m_2 that yield a plausible range of μ values (as in figs. B5-B6), the late-successional results are qualitatively similar to the plausible constant μ cases (e.g., figs. B1-B2).

Appendix C. Calculating leaf economics spectrum traits

Here, we describe how to calculate additional traits related to leaf economics from the two species-specific traits in our model, photosynthetic and structural leaf mass per area (LMA_p and LMA_s, respectively). Leaf lifespan (LL) is given by equation (A2). The annualized rate of leaf net photosynthesis (i.e., net assimilation, A, which is equal to gross photosynthesis minus maintenance respiration) at different light levels (L) is obtained on a leaf-area basis (g C assimilated m^{-2} leaf area yr^{-1}) by dividing equation (A3) (rate of net photosynthesis per-unit ground area) by leaf area index (LAI) and substituting in equations (A4)-(A6):

$$\frac{A(L)}{\text{area}} = P(L) - \frac{R}{LAI}$$
$$= \left(\frac{a_v LMA_p}{k_v + LMA_p} \right) \left(\frac{L}{k_p + L} \right) - \left(r_p LMA_p + r_s LMA_s \right). \tag{C1}$$

The mass-normalized form of this expression (g C assimilated g^{-1} leaf mass yr^{-1}) is obtained by dividing by LMA:

$$\frac{A(L)}{\text{mass}} = \frac{A(L)}{\text{area}} \, LMA^{-1}. \tag{C2}$$

Note that the annualized rates of assimilation (A) presented in this paper average over the diurnal cycle of radiation; therefore, the values we report differ quantitatively from instantaneous values reported in the literature (e.g., Wright et al., 2004). We evaluated equations (C1)-(C2) at two light levels: full sun ($L = 1$) to yield A_max/area and A_max/mass; and the late-successional equilibrium light level (L_eq) to yield A_eq/area and A_eq/mass. The light level L_eq is equivalent to the R^* concept of Armstrong and McGehee (1980) and Tilman (1982); i.e., L_eq is the understory light

level in the environment created by the late-successional competitively dominant species. We calculated L_{eq} in our model according to the solution in Appendix D (eq. [D9]) as follows:

$$L_{eq} = \frac{k_p\, z_1/z_2}{1 - (z_1/z_2)} \tag{C3}$$

where k_p is defined as in equation (A5), and z_1 and z_2 depend on the traits of the late-successional dominant species as follows:

$$z_1 = f_L\,(1 - f_R)\,\frac{r_p LMA_p + r_s LMA_s}{LMA_p + LMA_s} + (c_{LL}\,LMA_s)^{-1} + \mu \tag{C4}$$

$$z_2 = \left(\frac{f_L\,(1 - f_R)}{LMA_p + LMA_s}\right)\left(\frac{a_v\,LMA_p}{k_v + LMA_p}\right). \tag{C5}$$

In equations (C4)-(C5), LMA_p and LMA_s refer to the trait values of the late-successional dominant species, and other terms are defined in equations (A1)-(A6) and table A1.

Appendix D.   Mathematical details

In this appendix, we justify the claims that (i) it is appropriate to think about our system in terms of Tilman's R^* theory, meaning that there will be competitive exclusion (in the absence of disturbance) and the single surviving species will be the one that can sustain equilibrium with the lowest resource (light) level; (ii) for any given set of parameters, there exists a unique optimal allocation of resources of photosynthetic and structural tissue (LMA_p and LMA_s, respectively) for late-successional species; (iii) that this optimal (LMA_p, LMA_s) pair also maximize the function $(LL^{-1} + \mu)^{-1} A_{eq}/$mass (the mortality-adjusted lifetime return on investment in the late-successional understory light environment); and (iv) there is also a distinct unique optimal allocation for early-successional species. We assume a constant whole-plant mortality rate (μ) throughout this appendix, and we use the baseline value of μ (see table A1) for the numerical examples presented below. As explained in Appendix B, the model with constant μ can be re-parameterized to represent the case where μ depends on LMA_s. Thus, the mathematical proofs presented below apply equally to the main text and to the alternative mortality scenarios considered in Appendix B.

The model presented in Appendix A was developed as follows. The leaf biomass dynamics for species i can be expressed in terms of time-dependent model state variables (species biomasses $\vec{B}(t) = \{B_1(t), B_2(t), \ldots, B_n(t)\}$), global constants (non-species-specific parameters), and species-level traits ($LMA_{p,i}$ and $LMA_{s,i}$). To simplify the notation, we use the symbols $\vec{\rho} = (\rho_1, \rho_2, \ldots, \rho_n)$ to denote the collection of $LMA_{p,i}$ values, and $\vec{\sigma} = (\sigma_1, \sigma_2, \ldots, \sigma_n)$ for the $LMA_{s,i}$ values. Moreover, we will use the abbreviations $f := f_L (1 - f_R)$ and $c := c_{LL}$.

Using this notation, for example, if the current biomass distribution is summarized by the vector $\vec{B}$, and the various species have photosynthetic and structural mass allocations $\vec{\rho}$ and $\vec{\sigma}$, then total light availability in the system (eq. [A7]) can be written

$$L(\vec{B}; \vec{\rho}, \vec{\sigma}) = L_{\max} \exp\left(-\frac{1}{2} \sum_{i=1}^{n} \frac{B_i}{\rho_i + \sigma_i} \right), \tag{D1}$$

which is equivalent to the widely-used Beer-Lambert equation (Monsi and Saeki, 2005) with a decay constant of 0.5 (White et al., 2000). If $L_{\max} = 1$, then equation (D1) is equivalent to equation (A7). We will sometimes suppress the dependence of L on $\vec{\rho}$ and $\vec{\sigma}$.

In this section it will be important to think about how certain combinations of the parameters depend on the parameters ρ and σ. We can express the constants z_1 and z_2 introduced in equations (C4) and (C5) as functions of ρ and σ:

$$\zeta_1(\rho, \sigma) = f \frac{r_p \rho + r_s \sigma}{\rho + \sigma} + \frac{1}{c\sigma} + \mu \quad \text{and} \quad \zeta_2(\rho, \sigma) = \frac{f}{\rho + \sigma} \frac{a_v \rho}{k_v + \rho} \tag{D2}$$

where $z_1 = \zeta_1(\rho, \sigma)$ and $z_2 = \zeta_2(\rho, \sigma)$.

It is important to note that both of these are positive when both ρ and σ are positive. As indicated by equation (C3), it is the ratio of the two functions ζ_1 and ζ_2 that plays an essential role at equilibrium, so we introduce the function

$$\gamma(\rho, \sigma) = \frac{\zeta_1(\rho, \sigma)}{\zeta_2(\rho, \sigma)}. \tag{D3}$$

The two functions in equation (D2) play an essential role in determining the growth rate of a species given the current light availability (eq. [D1]). Indeed, suppose that the current light level

is given by the variable ℓ, then combining (A1) - (A6) with (D2) and (D3), we find that the growth rate of species i can be summarized as

$$u_i(\ell) = \zeta_2(\rho_i, \sigma_i)\left(\frac{\ell}{k_p + \ell}\right) - \zeta_1(\rho_i, \sigma_i). \tag{D4}$$

That is to say, the biomass dynamics of a full species system can be written in the simplified form

$$\frac{dB_i(t)}{dt} = B_i(t)\, u_i\big(L\big(\vec{B}(t)\big)\big). \tag{D5}$$

Modeling early- and late-successional species competition

The form of equation (D5) is useful because it provides a clear way to investigate what structural allocation properties are beneficial for species to have in early and late phases of succession.

In the context of the model, we consider the most competitive early-successional species to be the species with the maximum growth rate when light is at its maximum level (which is an approximation of conditions when the overall biomass is very close to zero.) That is to say, we investigate which species is the most competitive early-successional species in terms of the maximum growth rate, which, for a given pair of traits (ρ, σ), has the form

$$u_{\max}(\rho, \sigma) = \zeta_2(\rho, \sigma)\frac{L_{\max}}{k_p + L_{\max}} - \zeta_1(\rho, \sigma). \tag{D6}$$

It turns out that for the parameter values we considered, this function admits a unique maximum value. In the final subsection of this appendix we detail how this maximal pair, which we denote $(\tilde{\rho}, \tilde{\sigma})$, can be found numerically. Figures 1a and 3 compare the most competitive early-successional trait pair $(\tilde{\rho}, \tilde{\sigma})$ with the most competitive late-successional pair $(\hat{\rho}, \hat{\sigma})$, which is derived based on the $t \to \infty$ limit.

In contrast to early-successional competitive ability, which depends on performance under high light, late-successional competitive ability depends on performance under low light. As we demonstrate in the following section, the system (eq. [D5]) falls within the general framework studied by Armstrong and McGehee (1980). In theorem 1, we show that our system exhibits competitive exclusion. Consistent with the intuition set forth in Tilman's R^* theory, the most

competitive late-successional species is the one whose equilibrium point is associated with the lowest light (resource) level.

The most competitive late-successional species

The form of equation (D5) reveals that the growth rate for a species is zero when the function u_i is zero. Notice that since the functions ζ_1 and ζ_2 (eqs. [D2]) are both positive and do not depend on light level, it follows from equation (D4) that u_i is an increasing function with light availability. Moreover, in order for a species to be viable, it is at least necessary for the growth rate to be positive at the maximum light level. (Notice, on the other hand, a natural consequence of equation (D4) is that when $\ell = 0$, the growth rate is negative.) To guarantee that all species are viable if they were the only species in the environment, and to organize the species in a way that is useful later, we introduce the following assumption.

Assumption 1 (Viability at $L_{\max}$). *For each i, we assume that $\zeta_2(\rho_i, \sigma_i)L_{\max} > \zeta_1(\rho_i, \sigma_i)(k_p + L_{\max})$. Given this condition let the equilibrium light level ℓ_i^* be the (unique) value such that $u_i(\ell_i^*) = 0$. Furthermore, we assume that the species are organized such that $0 < \ell_1^* < \ell_2^* < \cdots < \ell_n^* < L_{max}$.*

We can relate this ℓ^* notation to the L_{eq} in equation (C3) as follows. Observe that for a given pair (ρ_i, σ_i), we can set the left-hand side of equation (D4) to zero and solve for ℓ to show that a species with a given pair of trait values (ρ_i, σ_i) will attain its equilibrium state at the light level

$$\ell_i^*(\rho_i, \sigma_i) = \frac{k_p \gamma(\rho_i, \sigma_i)}{1 - \gamma(\rho_i, \sigma_i)}. \tag{D7}$$

Recall that γ is the ratio of the growth and mortality functions ζ_2 and ζ_1 defined in equation (D2).

Finally, we can derive the biomass level associated with this equilibrium. Thinking of the light level L as a function of a vector of biomasses $\vec{b} = (b_1, b_2, \ldots, b_n)$, we note from equation (D1) that L is a decreasing function in each component b_i. Since $\lim_{b_i \to \infty} L(\vec{b}) = 0$, there is a unique b_i^* such that $L(0, \ldots, 0, b_i^*, 0, \ldots, 0) = \ell_i^*$. This is the biomass for this species at equilibrium if it is

the only species present, and the value is given by

$$b_i^* = 2(\rho_i + \sigma_i) \ln\left(\frac{L_{\max}}{\ell_i^*}\right). \tag{D8}$$

Given the preceding discussion and notation, we are ready to state our main mathematical results.

Theorem 1 (Armstrong and McGehee (1980))**.** *Suppose* $\{B_i(t)\}_{i=1}^n$ *and* L *satisfy equations (D1) - (D8) with parameters that satisfy Assumption 1. Then if the initial condition of the system satisfies* $B_1(0) > 0$, *we have that*

$$\lim_{t \to \infty} B_1(t) = b_1^*$$

$$\text{and } \lim_{t \to \infty} B_i(t) = 0, \text{ for } i = 2, 3, \ldots, n.$$

Proof. As is described in Appendix D of Armstrong and McGehee (1980), the theorem holds when two conditions are true. First, by Assumption 1, for each i there exists an $\ell_i^* > 0$ such that

$$u_i(\ell) \begin{cases} < 0, & \ell < \ell_i^* \\ = 0, & \ell = \ell_i^* \\ > 0, & \ell > \ell_i^* \end{cases}.$$

Second, for each i, $\frac{\partial L}{\partial b_i} < 0$, which completes the proof. $\square$

Given this theorem, the analysis reduces to finding the pair of values $(\hat{\rho}, \hat{\sigma})$ that produce the minimal light value. In fact, in the scenarios we have tested, the minimal pair is unique. The method reduces to using calculus.

As described above, for a given (ρ, σ), the minimal light level has the form (suppressing the dependence on the species index i)

$$\ell^*(\rho, \sigma) = \frac{k_p \gamma(\rho, \sigma)}{1 - \gamma(\rho, \sigma)} \tag{D9}$$

where γ is defined in equation (D3). Since ℓ^* is an increasing function in γ, it suffices to find a pair (ρ, σ) that minimizes γ. As such, we solved the partial derivatives of γ with respect to ρ and

σ separately and set each to zero. We then numerically computed the intersection

$$(\hat{\rho}, \hat{\sigma}) = \left\{ (\rho, \sigma) \,:\, \frac{\partial \gamma}{\partial \rho}(\rho, \sigma) = 0 \right\} \bigcap \left\{ (\rho, \sigma) \,:\, \frac{\partial \gamma}{\partial \sigma}(\rho, \sigma) = 0 \right\}$$

which can analytically be shown to be unique. This is the content of our next result, theorem 2.

Theorem 2. *Let $B(t)$ satisfy Equation (D5) with the number of species being $n = 1$. Then there exists a unique strictly positive pair of real numbers $(\hat{\rho}, \hat{\sigma})$ that achieve the minimal light value $L(B^*(\hat{\rho}, \hat{\sigma}))$.*

Proof. Without loss of generality, we set $L_{\max} = 1$.

Recall the fundamental quantity γ that needs to be minimized. First, we obtain the partial derivatives of γ with respect to ρ and σ:

$$\frac{\partial \gamma}{\partial \rho} = \frac{1}{\rho a_v} \left[-\frac{k_v}{\rho} \left(r_s \sigma + \frac{1}{f} + \frac{\mu \sigma}{f} \right) + \rho \left(r_p + \frac{1}{fc\sigma} + \frac{\mu}{f} \right) \right] \tag{D10}$$

$$\frac{\partial \gamma}{\partial \sigma} = \frac{k_v + \rho}{a_v \rho} \left[r_s + \frac{1}{fc\sigma} - \frac{\rho + \sigma}{fc\sigma^2} + \frac{\mu}{f} \right]. \tag{D11}$$

Next, we set each of the partial derivatives equal to zero and solve for the critical value $\hat{\rho}$ in terms of $\hat{\sigma}$. We begin with equation (D11):

$$\frac{\partial \gamma}{\partial \sigma} = 0 \iff r_s + \frac{1}{f\hat{\sigma}} - \frac{\hat{\rho} + \hat{\sigma}}{fc\hat{\sigma}^2} + \frac{\mu}{f} = 0. \tag{D12}$$

Solving for $\hat{\rho}$, we find that

$$\hat{\rho} = c\hat{\sigma}^2 \left(r_s f + \mu \right). \tag{D13}$$

Next, we set equation (D10) equal to zero and solve for ρ in terms of σ. First we find the least common denominator among the terms in the $\frac{\partial \gamma}{\partial \rho}$ equation, so we can write $\frac{\partial \gamma}{\partial \rho}$ as a single fraction.

$$\frac{\partial \gamma}{\partial \rho} = [r_p \rho^2 fc\sigma + r_s \sigma^2 \rho fc - r_s \sigma^2 k_v fc - r_s \sigma^2 \rho fc + \rho^2 + \rho\sigma$$

$$- k_v \sigma - \rho\sigma + \rho^2 c\sigma\mu + \rho c\mu\sigma^2 - c\mu\sigma^2 k_v - \rho c\mu\sigma^2] \big/ (a_v \rho^2 fc\sigma)$$

$$= [r_p \rho^2 fc\sigma - r_s \sigma^2 k_v fc + \rho^2 - k_v \sigma + \rho^2 c\sigma\mu - c\mu\sigma^2 k_v] \big/ (a_v \rho^2 fc\sigma)$$
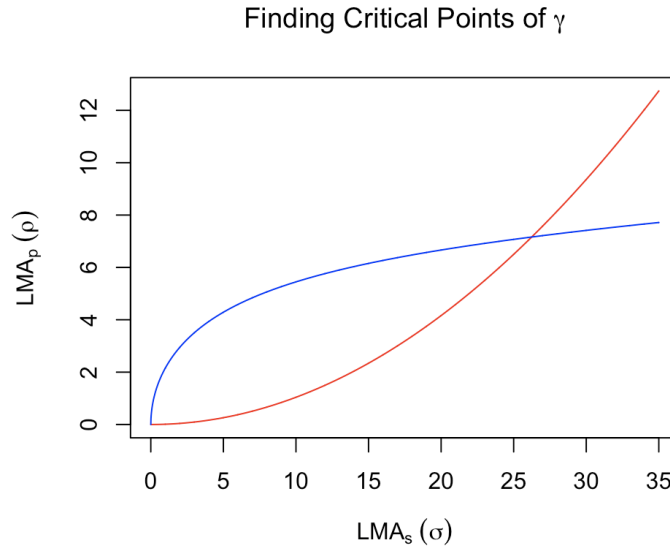
Figure D1: Demonstrating a key fact in the proof of theorem 2. We show that the function γ, defined by equation (D3), has a unique minimum with respect to the parameters ρ and σ. For any given value of σ, there exists a value of $\hat{\rho}_1(\sigma)$ such that $\frac{d\gamma}{d\rho}(\hat{\rho}_1(\sigma), \sigma) = 0$ (blue curve, eq. [D14]) and a separate value $\hat{\rho}_2(\sigma)$ such that $\frac{d\gamma}{d\sigma}(\hat{\rho}_2(\sigma), \sigma) = 0$ (red curve, eq. [D13]). Note that there exists only one nonzero $\hat{\sigma}$ such that $\hat{\rho}_1(\hat{\sigma}) = \hat{\rho}_2(\hat{\sigma})$, meaning that γ has a unique critical point for (ρ, σ) in the first quadrant.

As previously noted, when we set $\frac{\partial\gamma}{\partial\rho}$ equal to zero, we can simply set the numerator equal to zero, since we are assuming all of terms in the denominator are positive. Therefore

$$\frac{\partial\gamma}{\partial\rho} = 0 \iff r_p\hat{\rho}^2 fc\hat{\sigma} - r_s\hat{\sigma}^2 k_v fc + \hat{\rho}^2 - k_v\hat{\sigma} + \hat{\rho}^2 c\hat{\sigma}\mu - c\mu\hat{\sigma}^2 k_v = 0.$$

Solving for $\hat{\rho}$, we have

$$\hat{\rho} = \sqrt{\frac{\hat{\sigma}k_v(\hat{\sigma}fcr_s + 1 + \hat{\sigma}c\mu)}{\hat{\sigma}fcr_p + 1 + \hat{\sigma}c\mu)}}. \tag{D14}$$

The next step in solving for the values of $\hat{\rho}$ and $\hat{\sigma}$ that minimize light is to set equations (D13) and (D14) equal to each other and then solve for $\hat{\sigma}$. This cannot be achieved by hand; therefore, we turn to computational methods. A plot of equations (D13) and (D14) is shown in figure D1.

Parameter values from table A1 were used to generate this graph. The intersection point of the two lines represents the only critical point of γ (for these given parameter values). We will

now show that this critical point is the absolute minimum of γ. This would mean that the values of $\hat{\rho}$ and $\hat{\sigma}$ at the critical point represent the trait values that minimize light in our model.

To show this critical point is the absolute minimum of γ, we will solve for $\frac{\partial^2 \gamma}{\partial \rho^2}$, $\frac{\partial^2 \gamma}{\partial \sigma^2}$, and $\frac{\partial^2 \gamma}{\partial \sigma \partial \rho}$. Then we will show that $D = \frac{\partial^2 \gamma}{\partial \rho^2} \cdot \frac{\partial^2 \gamma}{\partial \sigma^2} - \left[\frac{\partial^2 \gamma}{\partial \sigma \partial \rho} \right]^2 > 0$ and $\frac{\partial^2 \gamma}{\partial \rho^2} > 0$.
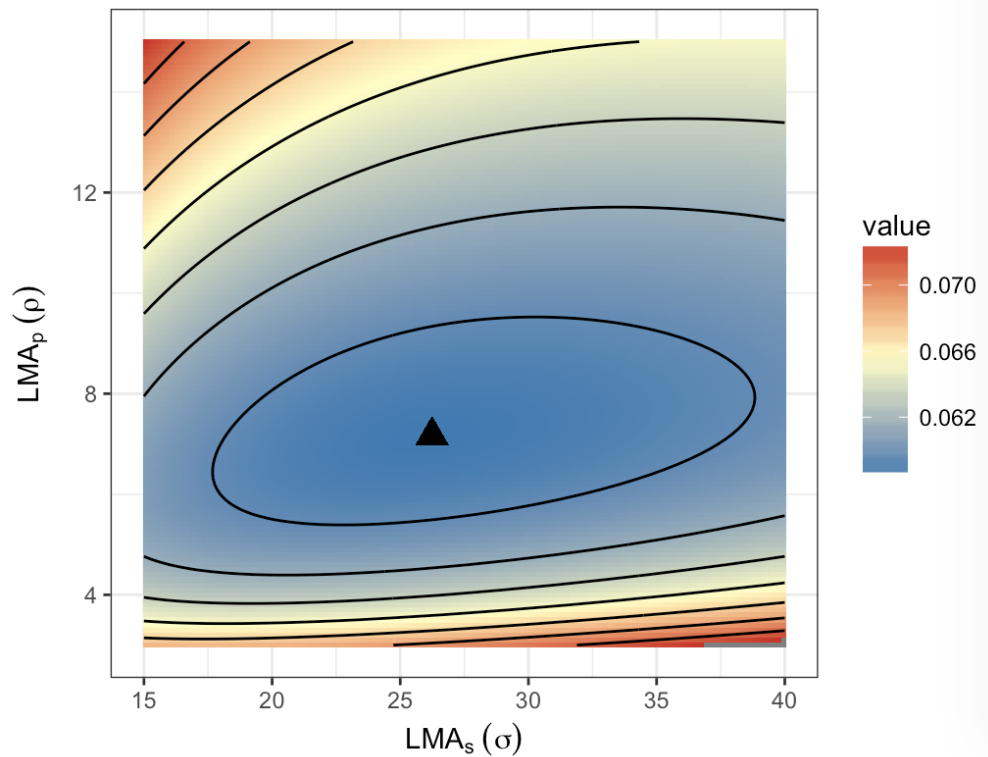

Figure D2: Demonstrating a key fact in the proof of theorem 2. This heatmap shows that the critical point of γ is a relative minimum. Recall: $LMA_{s,i}$ along the horizontal axis is represented by σ and $LMA_{p,i}$ along the vertical axis is represented by ρ.

□

To this end, a quick calculation shows that

$$\frac{\partial^2 \gamma}{\partial \rho^2} = \frac{2 \cdot k_v}{\rho^3 \cdot a_v} \left(r_s \sigma + \frac{1}{fc} + \frac{\mu \sigma}{f} \right) \tag{D15}$$

$$\frac{\partial^2 \gamma}{\partial \sigma^2} = \frac{2(k_v + \rho)}{\sigma^3 a_v fc} \tag{D16}$$

$$\frac{\partial^2 \gamma}{\partial \sigma \partial \rho} = -\frac{k_v}{\rho^2 a_v} \left(r_s + \frac{\mu}{f} + \frac{\rho^2}{\sigma^2 k_v fc} \right). \tag{D17}$$

It follows that

$$D = \frac{k_v}{\rho^3 a_v^2} \left[\frac{4(k_v + \rho)}{\sigma^3 fc} \left(r_s \sigma + \frac{1}{fc} + \frac{\mu \sigma}{f} \right) + \frac{k_v}{\rho} \left(r_s + \frac{\mu}{f} + \frac{\rho^2}{\sigma^2 k_v fc} \right)^2 \right]. \tag{D18}$$

Now, we note that, since all parameters are assumed to be greater than zero, we have $D > 0$ and $\frac{\partial^2 \gamma}{\partial \rho^2} > 0$. It follows that the intersection point in figure D1 is a relative minimum of γ.

In order to show that the critical point is an *absolute* minimum it remains to observe the following limits. Suppose $\rho > 0$, then $\lim_{\sigma \to \infty} \gamma(\rho, \sigma) = \infty$ and $\lim_{\sigma \to 0^+} \gamma(\rho, \sigma) = \infty$. Meanwhile, if $\sigma > 0$, then $\lim_{\rho \to \infty} \gamma(\rho, \sigma) = \infty$ and $\lim_{\rho \to 0^+} \gamma(\rho, \sigma) = \infty$.

Thus, we have shown that the critical point of γ (intersection point of fig. D1) is an absolute minimum. The heatmap displayed in figure D2 supports this claim.

The optimal late-successional species maximizes the lifetime return on investment

In Figure 3 we observed that, for the baseline parameter values (table A1), the optimal late-successional LMA_p and LMA_s pair coincides with the maximum of the mortality-adjusted lifetime return per-unit investment in leaf mass, $(LL^{-1} + \mu)^{-1} A_{\text{eq}}/\text{mass}$. In this section we will show that this holds in general.

Revisiting eqs. (C1) and (C2), which define $A_{\text{eq}}/\text{mass}$, and representing LMA_p and LMA_s by ρ and σ respectively, we can write the mass-normalized net assimilation rate at light-level L as follows:

$$\frac{A(L; \rho, \sigma)}{\text{mass}} = \frac{1}{\rho + \sigma} \left(\frac{a_v \rho}{k_v + \rho} \frac{L}{k_p + L} - (r_p \rho + r_s \sigma) \right). \tag{D19}$$

The specific value used for L in figure 3 is L_{eq}, which is the equilibrium light-level achieved for the optimal late-successional species. Recalling that leaf lifespan has the form $LL = c\sigma$ (where c is our shorthand in this appendix for c_{LL}), it follows that the full expression for the mortality-adjusted lifetime return on investment can be written

$$
\begin{aligned}
\mathcal{L}(\rho, \sigma) :&= (LL^{-1} + \mu)^{-1} \frac{A_{eq}}{\text{mass}} \\
&= \frac{1}{(\frac{1}{c\sigma + \mu})(\rho + \sigma)} \left(\frac{a_v \rho}{k_v + \rho} \frac{L_{eq}}{k_p + L_{eq}} - (r_p \rho + r_s \sigma) \right).
\end{aligned}
\tag{D20}
$$

where we have introduced the notation $\mathcal{L}(\rho, \sigma)$ to emphasize the dependence on LMA_p and LMA_s.

Proposition 3. *Let $\mathcal{L}(\rho, \sigma) = (LL^{-1} + \mu)^{-1} A_{eq}/\text{mass}$ be the mortality-adjusted leaf lifetime return on investment, as defined in equation (D20). Then the trait pair (LMA_p, LMA_s) that maximizes $\mathcal{L}$ is the same pair that gives the optimal late-successional strategy, which we denote $(\hat{\rho}, \hat{\sigma})$.*

Proof. First, recall that for a single species, the differential equation governing the biomass of that species can be written

$$
\frac{dB}{dt} = B(t)u(L(B(t))),
$$

where

$$
\begin{aligned}
L(B(t)) &= \exp\left(-\frac{1}{2} \frac{B(t)}{\rho + \sigma} \right); \\
u(\ell) &= \zeta_2(\rho, \sigma) \left(\frac{\ell}{k_p + \ell} \right) - \zeta_1(\rho, \sigma); \\
\zeta_1(\rho, \sigma) = f \frac{r_p \rho + r_s \sigma}{\rho + \sigma} + \frac{1}{c\sigma} + \mu; \quad &\text{and} \quad \zeta_2(\rho, \sigma) = \frac{f}{\rho + \sigma} \frac{a_v \rho}{k_v + \rho}.
\end{aligned}
\tag{D21}
$$

The constant f that appears in the last statement is $f = f_L(1 - f_R)$. See equations (D1)-(D5) for the original introduction of these quantities in the multi-species setting.

A species with $(LMA_p, LMA_s) = (\rho, \sigma)$ is in biomass equilbrium when the light level has reached a value ℓ^* which satisfies $u(\ell^*) = 0$. That is to say,

$$
0 = \zeta_2(\rho, \sigma) \frac{\ell^*}{k_p + \ell^*} - \zeta_1(\rho, \sigma).
$$

Recalling the notation $\gamma(\rho, \sigma) = \zeta_1(\rho, \sigma)/\zeta_2(\rho, \sigma)$ we see that ℓ^* must satisfy

$$\frac{\ell^*}{k_p + \ell^*} = \gamma(\rho, \sigma).$$

This quantity appears in equation (D20) with $\ell^* = L_{\text{eq}}$. Since L_{eq} is the equilibrium light level achieved by the optimal late-successional pair $\hat{\rho}, \hat{\sigma})$, we have the identity

$$\frac{L_{\text{eq}}}{k_p + L_{\text{eq}}} = \gamma(\hat{\rho}, \hat{\sigma}).$$

Comparing other terms that appear (D20) with the definitions for ζ_1 and ζ_2 in (D21), we see the following identities

$$\frac{1}{\rho + \sigma} \frac{a_v \rho}{k_v + \rho} = \frac{\zeta_2}{f}; \text{ and}$$

$$\frac{r_p \rho + r_s \sigma}{\rho + \sigma} = \frac{\zeta_1}{f} - \left(\frac{1}{c\sigma} + \mu \right).$$

It follows that

$$\mathcal{L}(\rho, \sigma) = \frac{1}{\frac{1}{c\sigma} + \mu} \left(\frac{\zeta_2(\rho, \sigma)}{f} \gamma(\hat{\rho}, \hat{\sigma}) - \frac{\zeta_1(\rho, \sigma)}{f} + \frac{1}{c\sigma} + \mu \right).$$

Note the appearance of $(\hat{\rho}, \hat{\sigma})$ in the factor with γ, which occurs because we are assessing this index function at L_{eq}. Now, factoring ζ_2/f from the first two terms in parentheses and recalling that $\gamma = \zeta_1/\zeta_2$ and then distributing the leading factor, we have

$$\mathcal{L}(\rho, \sigma) = \frac{1}{\frac{1}{c\sigma} + \mu} \left(\frac{\zeta_2(\rho, \sigma)}{f} \left(\gamma(\hat{\rho}, \hat{\sigma}) - \gamma(\rho, \sigma) \right) + \frac{1}{c\sigma} + \mu \right)$$

$$= \frac{\zeta_2(\rho, \sigma)}{f(\frac{1}{c\sigma} + \mu)} \left(\gamma(\hat{\rho}, \hat{\sigma}) - \gamma(\rho, \sigma) \right) + 1.$$

This form of the index $\mathcal{L}$ reveals why the maximum occurs at $(\hat{\rho}, \hat{\sigma})$. First, observe that if we plug in $(\hat{\rho}, \hat{\sigma})$ for (ρ, σ) we get the value 1. Since, by the findings in the previouis section, $(\hat{\rho}, \hat{\sigma})$ is the pair that minimizes the function γ, it follows that for all other choices, the quantity $\gamma(\hat{\rho}, \hat{\sigma}) - \gamma(\rho, \sigma)$ is negative. This implies that $\mathcal{L}(\rho, \sigma) < 1 = \mathcal{L}(\hat{\rho}, \hat{\sigma})$ when $(\rho, \sigma) \neq (\hat{\rho}, \hat{\sigma})$, which completes the proof. $\qquad \square$

The most competitive early-successional species

To simplify our notation, we let $\phi = u(L(0))$, which is a species' growth rate at the low-biomass (high-light) limit:

$$\phi = \frac{fa_v\rho}{(k_p+1)(\rho+\sigma)(k_v+\rho)} - \frac{f(r_p\rho+r_s\sigma)}{\rho+\sigma} - \frac{1}{c\sigma} - \mu. \tag{D22}$$

To solve for the optimal early-successional trait values (i.e., those that maximize ϕ), namely $\tilde{\rho}$ and $\tilde{\sigma}$, we will take the partial derivatives with respect to ρ and σ separately, set these derivatives equal to 0, solve for $\tilde{\sigma}$ in terms of $\tilde{\rho}$ in each case, set those two equations equal to each other and solve for $\tilde{\rho}$, and finally plug that expression for $\tilde{\rho}$ into either of our expressions for $\tilde{\sigma}$.

First, we solve for $\frac{d\phi}{d\rho}$:

$$\frac{d\phi}{d\rho} = \frac{fa_v(k_p+1)(\rho+\sigma)(k_v+\rho) - fa_v\rho(k_p+1)(2\rho+k_v+\sigma)}{\left[(k_p+1)(\rho+\sigma)(k_v+\rho)\right]^2}$$

$$- \left(\frac{fr_p(\rho+\sigma) - f(r_p\rho+r_s\sigma)}{(\rho+\sigma)^2}\right).$$

After finding a least common denominator and combining terms:

$$\frac{d\phi}{d\rho} = [fa_v(k_p+1)((\rho+\sigma)(k_v+\rho) - \rho(2\rho+k_v+\sigma)) - fr_p(\rho+\sigma)(k_p+1)^2(k_v+\rho)^2$$

$$+ fr_p(\rho+\sigma)(k_p+1)^2(k_v+\rho)^2] \cdot 1/[(k_p+1)(\rho+\sigma)(k_v+\rho)]^2. \tag{D23}$$

Next, we solve for $\frac{d\phi}{d\sigma}$:

$$\frac{d\phi}{d\sigma} = \frac{-fa_v\rho}{(k_p+1)(k_v+\rho)} \cdot \frac{1}{(\rho+\sigma)^2} - \left[\frac{fr_s(\rho+\sigma) - f(r_p\rho+r_s\sigma)}{(\rho+\sigma)^2}\right] + \frac{1}{c\sigma^2}.$$

After finding a least common denominator and combining terms:

$$\frac{d\phi}{d\sigma} = [-fa_v\rho c\sigma^2 - fr_s c\sigma^2(k_p+1)(\rho+\sigma)(k_v+\rho) + fc\sigma^2(r_p\rho+r_s\sigma)(k_p+1)(k_v+\rho)$$

$$+ (k_p+1)(\rho+\sigma)^2(k_v+\rho)] \cdot 1/[(k_p+1)(\rho+\sigma)^2(k_v+\rho)c\sigma^2]. \tag{D24}$$

Next, we set equations (D23) and (D24) equal to zero and solve for $\tilde{\sigma}$ in terms of $\tilde{\rho}$. Since all of our parameters are positive, we know the denominators of these two equations are positive,
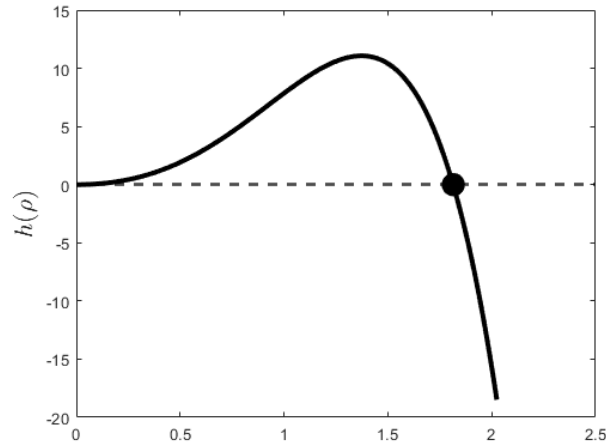
Figure D3: Recall that (ρ, σ) represents the trait pair (LMA_p, LMA_s). The function $h(\rho)$ comes from plugging the expression for $\tilde{\sigma}$ from equation (D25) into equation (D26). The only biologically sensible root of $h(\rho)$ is 1.77. The corresponding value of σ for this root is 0.66. Plugging this optimal pair $(\tilde{\rho}, \tilde{\sigma}) = (1.77, 0.66)$ into equation (D22) yields the greatest value of $\phi = 30.74$.

so we can simply set the numerators of these equations equal to zero and solve for $\tilde{\sigma}$ in terms of $\tilde{\rho}$.

Setting the numerator of equation (D23) equal to zero and solving for $\tilde{\sigma}$ in terms of $\tilde{\rho}$ yields the following expression:

$$\tilde{\sigma} = \frac{a_v \tilde{\rho}^2 + r_p(k_p + 1)(\tilde{\rho}^3 + 2\tilde{\rho}^2 k_v + \tilde{\rho}k_v^2) - r_p\tilde{\rho}(k_p + 1)(k_v + \tilde{\rho})^2}{a_v k_v - r_p k_v^2(k_p + 1) - r_p\tilde{\rho}^2(k_p + 1) + r_s(k_p + 1)(k_v + \tilde{\rho})^2 - 2r_p\tilde{\rho}k_v(k_p + 1)}. \tag{D25}$$

Now, setting the numerator of equation (D24) equal to zero and solving for $\tilde{\sigma}$ in terms of $\tilde{\rho}$, we have

$$0 = fc\tilde{\sigma}^2(r_p\tilde{\rho} + r_s\tilde{\sigma})(k_p + 1)(k_v + \tilde{\rho}) + (k_p + 1)(\tilde{\rho} + \tilde{\sigma})^2(k_v + \tilde{\rho})$$

$$- fr_s c\tilde{\sigma}^2(k_p + 1)(\tilde{\rho} + \tilde{\sigma})(k_v + \tilde{\rho}) - fa_v\tilde{\rho}c\tilde{\sigma}^2$$

This can be rewritten as a cubic equation in $\tilde{\sigma}$

$$
\begin{aligned}
0 = \ &\tilde{\sigma}^3 \big(fcr_s(k_p + 1)(k_v + \tilde{\rho}) \big) \\
&+ \tilde{\sigma}^2 \big(fcr_p\tilde{\rho}(k_p + 1)(k_v + \tilde{\rho}) + (k_p + 1)(k_v + \tilde{\rho}) \\
&\quad - fcr_s\tilde{\rho}(k_p + 1)(k_v + \tilde{\rho}) - fa_v c\tilde{\rho}) \big) \\
&+ \tilde{\sigma} \big(2\tilde{\rho}(k_p + 1)(k_v + \tilde{\rho}) \big) + \tilde{\rho}^2(k_p + 1)(k_v + \tilde{\rho}).
\end{aligned}
\tag{D26}
$$

Since we end up with a cubic in $\tilde{\sigma}$, we turn to computational methods to finish solving for the optimal values $\tilde{\rho}$ and $\tilde{\sigma}$. We will plug our expression for $\tilde{\sigma}$ from equation (D25) into equation (D26), and then solve for the roots of that equation, which we call $h(\rho)$. We then plug those values of ρ into equation (D25) to find the corresponding values of σ. Finally, since we are maximizing ϕ, we will plug the pairs of ρ and σ into equation (D22) to find the optimal pair $(\tilde{\rho}, \tilde{\sigma})$ that yields the greatest value.

The roots of $h(\rho)$ are $\rho = 0$, $\rho = 1.77$, $\rho = 49.97$, and $\rho = 52.98$. The only value that yields biologically sensible results is $\rho = 1.77$, which we have focused on in figure D3. The corresponding value of σ for this root is 0.66. Plugging this pair of ρ and σ into equation (D22) yields a result of $\phi = 30.74$.

So the optimal leaf mass allocations for an early-successional species (using the parameter values in table A1) are $\tilde{\rho} = 1.77$ and $\tilde{\sigma} = 0.66$. This result shows that compared to the optimal late-successional species (fig. D2), the optimal early-successional species has a relatively high ratio of LMA_p (ρ) to LMA_s (σ).

References

Armstrong, R. A., and R. McGehee. 1980. Competitive exclusion. American Naturalist 115:151–170.

Connell, J. H., and R. O. Slatyer. 1977. Mechanisms of succession in natural communities and their role in community stability and organization. American Naturalist 111:1119–1144.

Davies, S. J. 2001. Tree mortality and growth in 11 sympatric Macaranga species in Borneo. Ecology 82:920–932.

Monsi, M., and T. Saeki. 2005. On the factor light in plant communities and its importance for matter production. Annals of Botany 95:549–567.

Pacala, S. W., C. D. Canham, J. Saponara, J. A. Silander, R. K. Kobe, and E. Ribbens. 1996. Forest models defined by field measurements: estimation, error analysis and dynamics. Ecological Monographs 66:1–43.

Poorter, L., and F. Bongers. 2006. Leaf traits are good predictors of plant performance across 53 rain forest species. Ecology 87:1733–1743.

Reich, P. B., D. S. Ellsworth, and C. Uhl. 1995. Leaf Carbon and Nutrient Assimilation and Conservation in Species of Differing Successional Status in an Oligotrophic Amazonian Forest. Functional Ecology 9:65–76.

Stephenson, N. L., P. J. van Mantgem, A. G. Bunn, H. Bruner, M. E. Harmon, K. B. O'Connell, D. L. Urban, et al. 2011. Causes and implications of the correlation between forest productivity and tree mortality rates. Ecological Monographs 81:527–555.

Tilman, D. 1982. Resource competition and community structure. Princeton University Press, Princeton, NJ.

White, M. A., P. E. Thornton, S. W. Running, and R. R. Nemani. 2000. Parameterization and sensitivity analysis of the BIOME-BGC terrestrial ecosystem model: net primary production controls. Earth Interactions 4, paper 3:1–85.

Wright, I. J., P. B. Reich, M. Westoby, D. D. Ackerly, Z. Baruch, F. Bongers, J. Cavender-Bares, et al. 2004. The worldwide leaf economics spectrum. Nature 428:821–827.

Wright, S. J., K. Kitajima, N. J. Kraft, P. B. Reich, I. J. Wright, D. E. Bunker, R. Condit, et al. 2010. Functional traits and the growth-mortality trade-off in tropical trees. Ecology 91:3664–3674.